RESEARCH ARTICLE SUMMARY

STRATOSPHERIC OZONE

Rapid ozone depletion after humidification of the stratosphere by the Hunga Tonga Eruption

Stephanie Evan*, Jerome Brioude, Karen H. Rosenlof, Ru-Shan Gao, Robert W. Portmann, Yunqian Zhu, Rainer Volkamer, Christopher F. Lee, Jean-Marc Metzger, Kevin Lamy, Paul Walter, Sergio L. Alvarez, James H. Flynn, Elizabeth Asher, Michael Todt, Sean M. Davis, Troy Thornberry, Holger Vömel, Frank G. Wienhold, Ryan M. Stauffer, Luis Millán, Michelle L. Santee, Lucien Froidevaux, William G. Read

INTRODUCTION: The Hunga Tonga–Hunga Ha'apai (HT) underwater volcanic eruption of 15 January 2022 was exceptional in that it injected more water (H_2O) vapor than has ever been observed in the satellite era. A rapid response was initiated that provided the data needed to explore the early chemical effects of this rare event. Volcanic eruptions inject gases and particles into the stratosphere, potentially influencing climate and ozone (O_3) chemistry. Understanding the intricate connections between volcanic emissions and atmospheric chemistry and their broader implications is vital for advancing our capabilities of modeling environmental processes.

RATIONALE: Our research provides new insights into the initial effects of the HT eruption on stratospheric composition. This eruption was notable for injecting material, including an unprecedented amount of H_2O vapor (10% of the total global mean stratospheric burden), to very high altitudes (up to 55 km). Using observational data, we investigated the speed of impacts and potential influence on stratospheric bromine and chlorine species, nitrogen oxide (NO), as well as O_3.

RESULTS: Our study combined balloon measurements, zenith sky observations, and satellite data to capture the early evolution of the HT volcanic plume's impact on O_3. In just 1 week, the stratospheric O_3 above the tropical southwestern Pacific and Indian Ocean region decreased by 5%. This change gains context when compared with the Antarctic O_3 hole, where up to 60% of the O_3 is depleted from September to November. This tropical O_3 decrease exceeds that of previous eruptions, underscoring the HT event's exceptional nature.

H_2O vapor played a pivotal role in consequences of the HT event. Its increased abundance resulted in higher relative humidity and radiative cooling in the stratosphere, enabling chemical reactions on the surfaces of volcanic aerosols to occur at temperatures warmer than their typical range. These chemical processes on hydrated volcanic aerosols led to the formation of active chlorine species such as chlorine monoxide (ClO) from inactive chlorine (hydrogen chloride, HCl). Combined with a decrease in nitrogen oxides (NOx), these active chlorine species catalytically destroyed O_3 molecules. The decrease in hydrogen chloride (HCl) by 0.4 parts per billion by volume (ppbv) and the increase in ClO by 0.4 ppbv provided compelling evidence for chlorine activation, leading to rapid O_3 destruction within this volcanic plume.

The experimental data reveal the processes behind the observed O_3 depletion, unveiling the intricate interplay between this volcano's emissions and perturbed stratospheric chemistry. Enhanced humidity, radiative cooling, and expanded aerosol surface area in the plume created ideal conditions for rapid chlorine activation on hydrated volcanic aerosols at warm temperatures and subsequent O_3 depletion.

CONCLUSION: Our study sheds light on the complex interactions between a large volcanic eruption and tropical stratospheric O_3, bridging a large gap in our knowledge. The HT eruption's unusual features, notably its high injection altitude of aerosol precursors and large amounts of H_2O vapor, yield invaluable insights into stratospheric chemistry perturbations after this major event.

Beyond its volcanic relevance, our research offers crucial insights into atmospheric chemistry and its implications for climate change. The comprehensive observational evidence that we present substantially advances our understanding of rapid O_3 depletion in certain volcanic plumes. Our study also provides new perspectives on the effects of volcanic eruptions on stratospheric composition and informs future studies and early-response strategies to assess their aftermath. ■

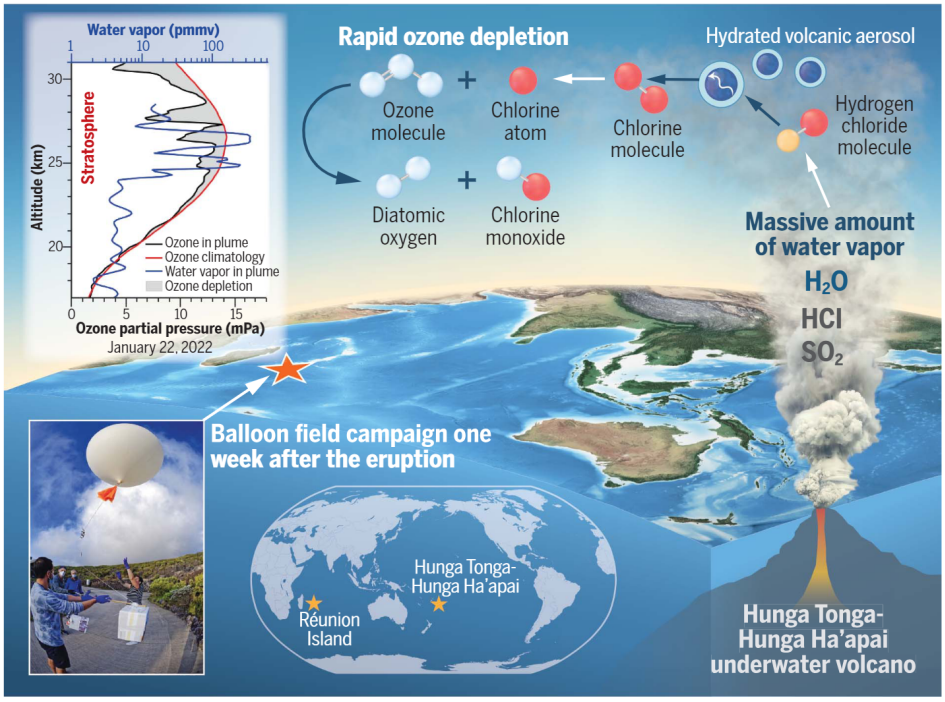

Eruption-triggered rapid O_3 depletion. After the HT eruption, a balloon campaign took place at Réunion Island (left picture). Plume dynamics showcase the volcanic injection of H_2O vapor, sulfur dioxide (SO_2), and HCl, prompting rapid chlorine activation on hydrated volcanic aerosol and O_3 depletion in the stratosphere. The 22 January 2022 O_3 profile (black line) contrasts with Réunion's climatology (red line), displaying a notable decline.

The list of author affiliations is available in the full article online.

*Corresponding author. Email: stephanie.evan@univ-reunion.fr

Cite this article as S. Evan *et al.*, *Science* **382**, eadg2551 (2023). DOI: 10.1126/science.adg2551

READ THE FULL ARTICLE AT
https://doi.org/10.1126/science.adg2551

RESEARCH ARTICLE

STRATOSPHERIC OZONE

Rapid ozone depletion after humidification of the stratosphere by the Hunga Tonga Eruption

Stephanie Evan[1]*, Jerome Brioude[1], Karen H. Rosenlof[2], Ru-Shan Gao[2], Robert W. Portmann[2], Yunqian Zhu[2,3], Rainer Volkamer[4], Christopher F. Lee[4], Jean-Marc Metzger[5], Kevin Lamy[1], Paul Walter[6], Sergio L. Alvarez[7], James H. Flynn[7], Elizabeth Asher[2,3], Michael Todt[8], Sean M. Davis[2], Troy Thornberry[2], Holger Vömel[9], Frank G. Wienhold[10], Ryan M. Stauffer[11], Luis Millán[12], Michelle L. Santee[12], Lucien Froidevaux[12], William G. Read[12]

The eruption of the Hunga Tonga–Hunga Ha'apai volcano on 15 January 2022 offered a good opportunity to explore the early impacts of tropical volcanic eruptions on stratospheric composition. Balloon-borne observations near Réunion Island revealed the unprecedented amount of water vapor injected by the volcano. The enhanced stratospheric humidity, radiative cooling, and expanded aerosol surface area in the volcanic plume created the ideal conditions for swift ozone depletion of 5% in the tropical stratosphere in just 1 week. The decrease in hydrogen chloride by 0.4 parts per million by volume (ppbv) and the increase in chlorine monoxide by 0.4 ppbv provided compelling evidence for chlorine activation within the volcanic plume. This study enhances our understanding of the effect of this unusual volcanic eruption on stratospheric chemistry and provides insights into possible chemistry changes that may occur in a changing climate.

Large, explosive volcanic eruptions can affect the climate by injecting gases such as sulfur dioxide (SO_2), water vapor (H_2O), and carbon dioxide (CO_2) and halogen compounds such as hydrochloric acid (HCl) and hydrobromic acid (HBr) into the stratosphere. Typically, sulfate aerosols form from sulfur dioxide (SO_2) on a timescale of 1 month (*1*). These aerosols cool the surface by reflecting some incoming solar radiation and warm the stratosphere through the absorption of long-wave radiation. Sulfate aerosol heating can alter stratospheric transport, affecting the distribution of stratospheric species (*1*). The increase in the aerosol burden also enhances aerosol surface area density, increasing the rate of heterogeneous chemical reactions that play a role in stratospheric ozone (O_3) chemistry.

Previous volcanic eruptions had a noticeable impact on stratospheric O_3; examples include El Chichón in 1982 (*2*, *3*) and Mt. Pinatubo in 1991 (*4*, *5*). After the eruption of Mt. Pinatubo, the total O_3 column was reduced by ~6% in northern polar and midlatitude regions (*6*). The O_3 was destroyed by chemical reactions on volcanic aerosols transported to high latitudes, which provided additional reactive surface area for the same heterogeneous chemical reactions that cause polar O_3 loss each year. In the tropics, a 6% decrease in total O_3 was observed in satellite and ozonesonde data (*7*). It was confined between 24 and 28 km in altitude and started 1 month after the eruption, consistent with the time needed for SO_2 to be converted to sulfate aerosols (*8*).

To assess the atmospheric impacts of volcanic eruptions, in situ observations of H_2O vapor, aerosol size and concentration, trace gases (e.g., O_3 and chlorinated species), and meteorological conditions (e.g., temperature and winds) after the eruptions are important (*9*). Major eruptions that cause large perturbations to the aerosol loading and O_3 chemistry of the stratosphere occur sporadically, so the opportunity to make in situ measurements in these plumes is rare.

The Hunga Tonga–Hunga Ha'apai submarine volcano (hereafter HT) in the tropical South Pacific (20.55°S, 175.38°W) was the largest volcanic eruption in the past 30 years. The massive eruption on 15 January 2022 sent material as high as 50 to 55 km, the greatest height ever seen by satellites for a volcanic plume (*10*, *11*). Satellite measurements indicated that the HT volcano injected into the stratosphere a relatively small amount of SO_2, 0.4 Tg (*11*), compared with 10 to 20 Tg from Mt. Pinatubo (*12*, *13*). However, unlike past eruptions, it injected a massive amount of H_2O [~150 Tg, or 10% of the total global mean stratospheric burden (*11*)]. The large amount of injected H_2O was confirmed by radiosonde in situ measurements (*14*).

Less than 1 week after the eruption, a rapid response balloon campaign took place at the Maïdo Observatory (MO) in Réunion Island (21°S, 55°E) (*15*). Because of zonal easterly winds in the stratosphere (20 to 50 km), Réunion Island was ideally located downwind of the plume. From 20 to 24 January 2022, multiple meteorological balloons carrying aerosol, H_2O, SO_2, and O_3 instruments were launched each night to provide key measurements of the volcanic plume's composition (see the materials and methods). A field campaign resulting in volcanic plume measurements in the stratosphere by in situ instruments has never occurred this quickly after an eruption; as a comparison, a rapid response balloon campaign was deployed to Hawaii within 15 days of the 2018 Kilauea eruption (*9*). Herein, we present unprecedented observations corroborating the occurrence of fast chemical depletion of O_3 inside the volcanic plume in the week after the HT eruption. The extremely high H_2O vapor values accelerated the oxidation of SO_2 to sulfate aerosols, with much of the conversion in the densest parts of the plume occurring within a few days after the eruption (*16*), thus facilitating heterogeneous chemical O_3 loss. Additionally, as noted by Anderson *et al.* (*17*), high stratospheric H_2O vapor can change the catalytic chlorine free radical chemistry by shifting total available inorganic chlorine (principally HCl and chlorine nitrate, $ClONO_2$) into the catalytically free-radical form, ClO, potentially increasing O_3 loss. Both rapid aerosol conversion and additional O_3 loss appeared very rapidly for the HT eruption. The high vertical resolution in situ measurements were critical for observing this loss, which is not easily apparent in the satellite O_3 observations, which smear features in the vertical.

Results

Balloon-borne profiles of O_3 and H_2O vapor

Figure 1 shows the balloon-borne profiles of O_3 and H_2O at MO for the period 20 to 24 January 2022. It took 6 days for the volcanic plume to reach Réunion at an ~30-km altitude. Balloon measurements 5 days after the eruption indicate typical stratospheric background values of H_2O (4.5 ppmv), an unperturbed Junge layer backscatter signal, and a peak in O_3 partial pressure of 15 mPa at 25 km. At Réunion, the highest observed H_2O mixing ratio of 356 ppmv at 27 km, 21 Coordinated Universal Time (UTC), was reported on 22 January 2022. Larger values near 1000 ppmv were seen in radiosonde measurements closer to the eruption by Vömel *et al.* (*14*). The observed progression of descending altitude with time in

[1]Laboratoire de l'Atmosphère et des Cyclones (LACy), UMR8105, CNRS, Université de La Réunion, Météo-France, Saint-Denis, France. [2]NOAA Chemical Sciences Laboratory, Boulder, CO, USA. [3]Cooperative Institute for Research in Environmental Sciences, University of Colorado, Boulder, CO, USA. [4]Department of Chemistry and Cooperative Institute for Research in Environmental Sciences, University of Colorado, Boulder, CO, USA. [5]Observatoire des Sciences de l'Univers de la Réunion, UAR 3365 (CNRS, Université de la Réunion, Météo-France), Saint-Denis, France. [6]St. Edward's University, Austin, TX, USA. [7]University of Houston, Houston, TX, USA. [8]Finnish Meteorological Institute, Helsinki, Finland. [9]National Center for Atmospheric Research, Boulder, CO, USA. [10]Swiss Federal Institute of Technology (ETH), Zurich, Switzerland. [11]Atmospheric Chemistry and Dynamics Laboratory, NASA Goddard Space Flight Center, Greenbelt, MD, USA. [12]Jet Propulsion Laboratory, California Institute of Technology, Pasadena, CA, USA.
*Corresponding author. Email: stephanie.evan@univ-reunion.fr

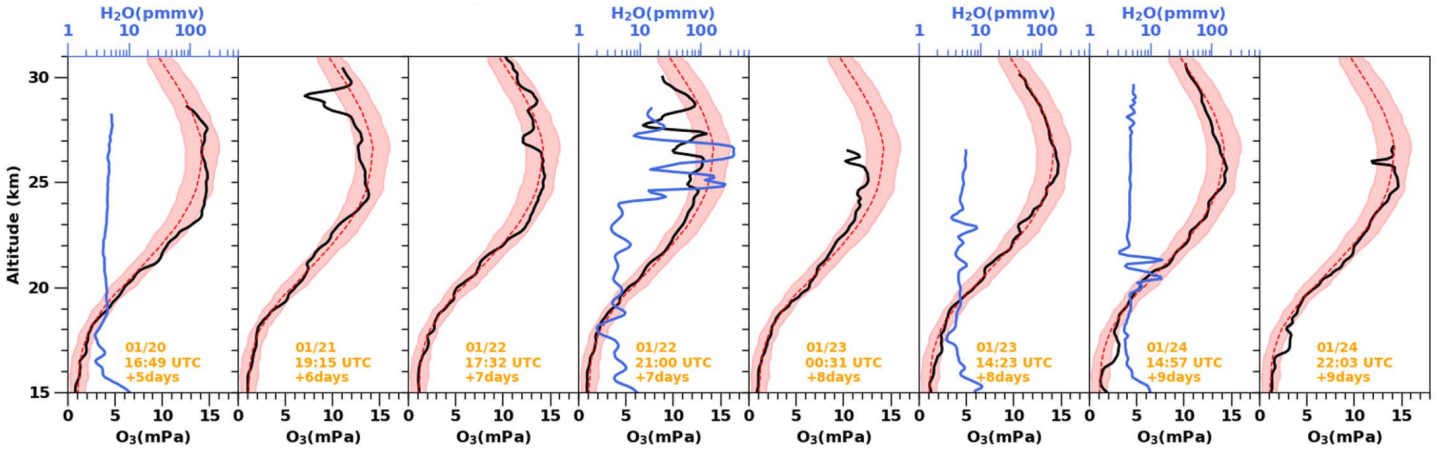

Fig. 1. Soundings of O_3 and H_2O vapor 1 week after the eruption. Profiles of O_3 partial pressure (black) and H_2O vapor mixing ratio (blue) measured at MO on Réunion Island over the period 20 to 24 January 2022. SHADOZ climatological O_3 partial pressure for January for Réunion Island is indicated by the red dashed line. The red shaded area shows values ±1 SD above and below the mean.

the peak of the H_2O plume in Fig. 1 can be explained by the vertical sheer in easterly zonal winds. The easterly zonal winds linearly decreased from 30 m s^{-1} at 30 km to 20 m s^{-1} at 20 km, causing the plume to travel ~18° in longitude per day (*11*, *14*).

The largest O_3 decrease was observed on 21 and 22 January at 25 to 29 km. The decrease amounted to a loss of 10 to 45% relative to O_3 climatology from 1998 to present (see the materials and methods). The presence of SO_2 inside the volcanic plume could affect the performance of electrochemical concentration cell (ECC) ozonesondes by decreasing the sensor signal, resulting in artificially low O_3 measurements. During the experiment, SO_2 instruments (*18*) were launched in tandem with ECC ozonesondes on three flights (see the materials and methods). Overall, the data indicate that SO_2 interference contributes to only a small negative bias of 3 to 4% in the O_3 decrease observed at >25 km in the week after the eruption (see the materials and methods).

Satellite measurements of gas-phase constituents

Satellite measurements of stratospheric gas profiles from the Aura Microwave Limb Sounder (MLS), in operation since 2004 (*19*), were also used to diagnose the possible mechanisms of O_3 decrease after the eruption. Because MLS measures microwave thermal emission from the Earth's limb, its retrievals are largely unaffected by the presence of volcanic aerosols that strongly impair visible, ultraviolet, and infrared measurements. MLS observed the massive H_2O perturbation, as well as anomalous values of several trace gases injected into the stratosphere by HT, such as SO_2 and HCl (*11*). Large H_2O values >100 SDs (σ) above background levels were observed in the week after the eruption at between 20 and 30 km, with a maximum value as high as 350 ppmv at 30 km on 16 January 2022. As shown in Fig. 2, MLS measurements of O_3, HCl, and ClO radicals inside the volcanic plume were identified by selecting data points with H_2O vapor mixing ratios >10 ppmv between 100 and 10 hPa (see the materials and methods). Then, for each data point, the climatological average profile for the month of January from 1998 to 2021 was computed by using MLS profiles in a 5° × 5° box region around the point (see the materials and methods). MLS O_3 mixing ratios inside the volcanic plume decreased at 18 to 21 hPa (~27 to 28 km) in the week after the HT eruption, from an average value of 6.3 ppmv on 16 January 2022 to a minimum value of 4.6 ppmv on 20 January 2022 (near 18°S, 88°E) at 21 hPa, which is 27% below climatological values.

Sensitivity of O_3 decrease to H_2O conditions

We computed average O_3 anomaly and SE profiles inside the plume for the period 16 to 24 January 2022 for two H_2O thresholds, 10 and 100 ppmv, to assess the sensitivity of stratospheric O_3 decrease to H_2O conditions (Fig. 2C). The decrease in MLS O_3 was more pronounced for higher H_2O mixing ratios, and the largest average O_3 drop of 0.4 ppmv (SE of 0.04 ppmv) at 28 km was observed for profiles with H_2O mixing ratios >100 ppmv. Thirty percent of the 190 O_3 profiles selected using the 100 ppmv H_2O mixing ratio threshold showed O_3 dropping below 0.5 ppmv. This change is larger than the typical range of variability established by MLS O_3 measurements for the month of January from 2005 to 2021 period (SD = 0.25 ppmv) or the 2-σ uncertainty of individual MLS O_3 data points (0.1 ppmv) (*20*).

The average O_3 decrease in the ozonesonde profiles was 0.6 ppmv (SE = 0.25 ppmv) near 27 to 29 km, and the strongest decrease was observed during the night of 22 January 2022, when H_2O vapor mixing ratios were the highest. Thus, the large quantity of H_2O vapor injected by the HT volcano appears to have played a key role in the stratospheric O_3 decrease observed by both ozonesondes and MLS.

Discussion

Comparing the HT eruption with that of Mt. Pinatubo

The June 1991 Mt. Pinatubo eruption had a substantial impact on the tropical O_3 column, resulting in a reduction of 13 to 20 Dobson units (DU) within 3 to 6 months (*7*, *8*). This O_3 decrease is comparable to the 18.3 DU loss observed in the 22 January 2022 O_3 profile, but the latter occurred much more rapidly after the HT eruption, indicating the involvement of different mechanisms. The observed low O_3 levels in the tropics after the Mt. Pinatubo eruption were likely caused by increased tropical upwelling due to the heating of volcanic aerosols, facilitating the vertical transport of O_3-depleted air from the troposphere to the stratosphere (*4*). However, the magnitude of O_3 decrease observed after the HT eruption cannot be attributed to lofting, because the radiative cooling effect of the injected H_2O into the stratosphere offset the heating caused by volcanic aerosols (*21*).

Understanding O_3 changes in the tropical stratosphere

A volcanic plume ascending into the stratosphere can incorporate O_3-poor tropospheric air and lead to a localized reduction in column O_3. This effect would have been most prominent in the initial observations of the plume by MLS on 16 January 2022, and over time, the dilution of the volcanic plume would have diminished this apparent loss. However, the minimum O_3 levels were observed at 27 to 28 km altitude 5 days after the eruption, indicating that chemistry played a more prominent role in the observed O_3 changes.

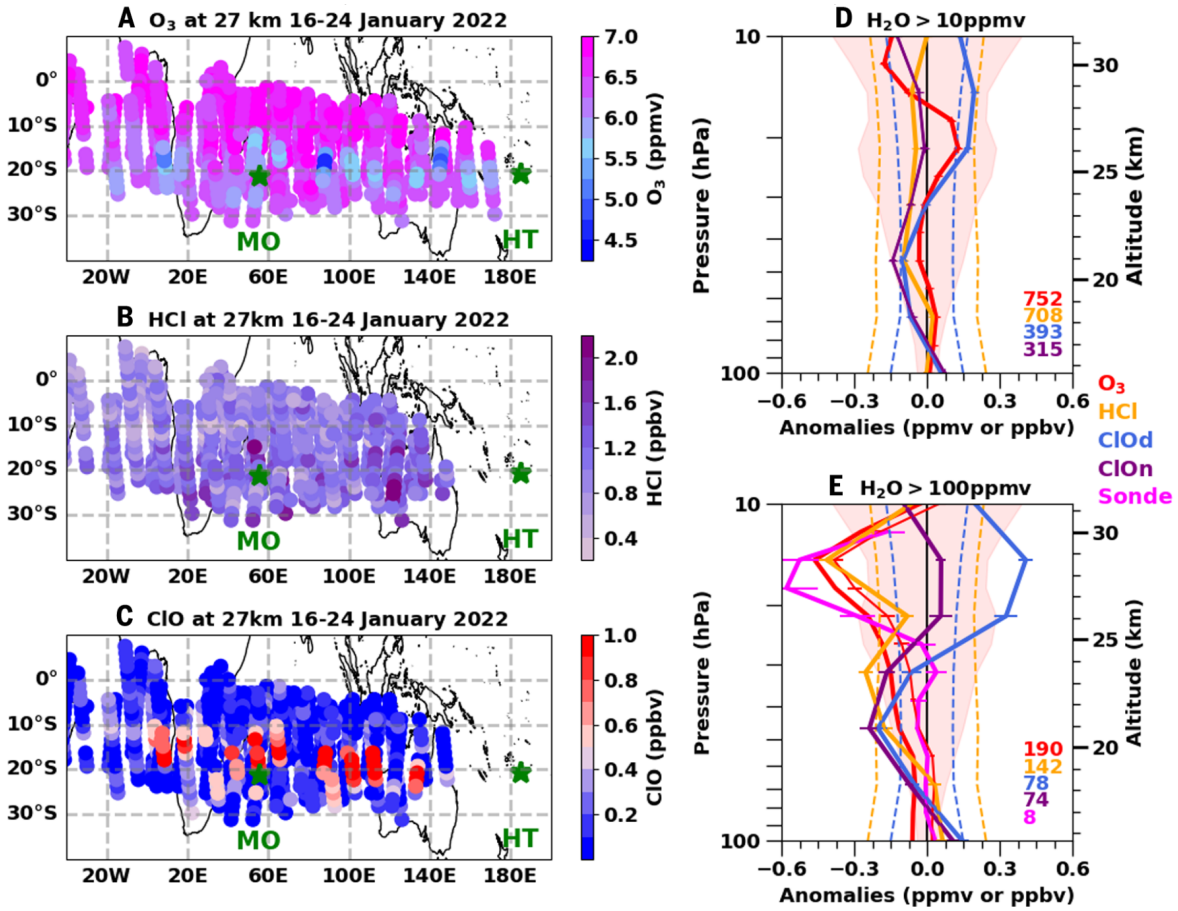

Fig. 2. MLS satellite measurements inside the volcanic plume. (**A** to **C**) MLS maps of O_3 (A), HCl (B), and ClO (C) at 27 km for the period 16 to 24 January 2022. The locations of HT and MO are indicated by green stars. Colored circles correspond to individual satellite profiles. (**D**) MLS anomaly profiles (see the materials and methods) of O_3 (in ppmv; red), HCl (in ppbv; orange), and ClO (in ppbv; blue and purple) inside the volcanic plume averaged over the period 16 to 24 January 2022. Anomalies were computed for MLS measurements inside the plume using a H_2O vapor threshold of 10 ppmv. (**E**) Same as (D) for but H_2O mixing ratios exceeding 100 ppmv. The red shaded area in (D) and (E) indicate ±1 SD of the O_3 climatology. In (E), the average O_3 anomaly profile measured by the balloon sondes in Réunion Island is shown in magenta (ozonesonde data degraded to MLS vertical resolution; see the materials and methods). In (D) and (E), the dashed orange lines correspond to ±1 SD of the HCl climatology, and the dashed blue lines correspond to ±1 SD of the ClO climatology; numbers indicate how many profiles were used to compute the average anomaly. For ClO, the averaged anomaly profiles were computed for daytime (blue) and nighttime (purple) ClO measurements.

The O_3 depletion within the HT volcanic plume exceeded rates observed in previous major eruptions such as El Chichòn and Mt. Pinatubo. Less than 1 week after the HT eruption, O_3 decreased by 0.5 ppmv (i.e., ~0.07 ppmv per day) between 25 and 29 km altitude. The largest seasonal stratospheric O_3 depletion occurs in the polar regions, specifically over the Arctic and Antarctica (*22*). Over the winter months (January to April) in the Arctic, O_3 depletion estimates range from 0.2 to 1.9 ppmv, whereas in Antarctica during the corresponding season, O_3 loss estimates range from 2.3 to 3 ppmv (*23*). These O_3 loss estimates are much larger than the one observed after the HT eruption, although polar O_3 depletion spanned a longer period of 3 to 4 months. During the formation of the Antarctic O_3 hole, stratospheric O_3 is destroyed at a maximum rate of 0.08 ppmv per day (*24*), which is comparable to the rate of 0.07 ppmv per day observed after the HT eruption. Although the comparison involves processes occurring in different regions, it provides valuable context to underscore the substantial and swift O_3 loss observed after the HT eruption.

The stratospheric chemistry behind O_3 depletion

Both gas-phase and heterogeneous chemistry play substantial roles in understanding O_3 depletion in the stratosphere (*22*). Gas-phase chemistry involves a complex suite of reactions between O_3 and various catalytic cycles, notably hydrogen (HOx: hydroxyl radical OH and perhydroxyl radical HO_2), nitrogen (NOx: nitrogen monoxide NO and nitrogen dioxide NO_2), chlorine (ClOx: chlorine Cl and chlorine monoxide ClO), and bromine (BrOx: bromine Br and bromine monoxide BrO) oxides (see the materials and methods). The chemistry involving NOx is closely intertwined with that of halogens (ClOx and BrOx) and of HOx (see the materials and methods).

Reactive halogens, such as chlorine (ClO, Cl) and bromine (BrO, Br) species, have been identified as significant agents in O_3 depletion (*25*). Brominated species, in the presence of elevated Cl, demonstrate higher O_3 destruction efficiency compared with chlorine species due to their longer reaction chains (*26*). The generation of reactive halogen gases involves the transformation of halogen reservoir source gases (HCl, $ClONO_2$, HBr, and $BrONO_2$). Photolysis plays a key role in dissociating bromine reservoir species (HBr, $BrONO_2$), whereas chlorine reservoir species (HCl, $ClONO_2$) undergo relatively slow photolysis in the gas phase. However, more rapid transformations occur through heterogeneous reactions on solid or liquid particle surfaces (see the materials and methods).

Heterogeneous chlorine chemistry has been well established in polar regions, where polar stratospheric clouds form at temperatures below ~195 K. These clouds, along with cold sulfate particles, play a crucial role in the conversion of inorganic chlorine species ($ClONO_2$ and HCl) into chemically active forms of chlorine, namely ClO and Cl (*22*), which subsequently initiate catalytic O_3 loss in the polar regions. Activation of $ClONO_2$ and HCl through heterogeneous reactions becomes more efficient as temperature decreases or as increased H_2O dilutes the H_2SO_4 concentration (*27*).

Some volcanic eruptions have been observed to emit halogens such as HCl and HBr into the stratosphere, along with SO_2 (*28*). Halogens, particularly HCl, are highly soluble and can be scavenged by H_2O, ice hydrometeors, and ash present in the volcanic plume (*29*). Theoretical predictions and advanced plume models indicate that 10 to 20%, of the HCl emitted at the vent during large, explosive volcanic eruptions could directly reach the stratosphere (*28*). Thus, observational examples of significant HCl and HBr emissions from volcanic events that directly lead to stratospheric O_3 depletion are limited (*30*). Depletion of stratospheric O_3 observed after volcanic eruptions has been mainly attributed to heterogeneous reactions occurring on volcanic sulfate aerosols, based on modeling studies [e.g., (*2*, *31*)]. Furthermore, the increased presence of stratospheric sulfate aerosols resulting from volcanic eruptions can also lead to a reduction in the abundance of NOx (*32*), making the ClOx and HOx cycles more effective at destroying O_3 (see the materials and methods). If less NOx is available, then the catalytic O_3 depletion through NOx could slow down. However, this effect has primarily been observed at higher altitudes (>30 km) after the Mt. Pinatubo eruption (*33*).

Although the impact of volcanic eruptions on O_3 depletion in midlatitude regions is relatively well documented [e.g., (*4*, *34*)], there have been fewer studies that specifically focus on the effects of volcanic eruptions and heterogeneous chemistry on the distribution of stratospheric O_3 in tropical regions, because most volcanic injections do not reach altitudes high enough to substantially influence stratospheric O_3 chemistry in the tropics. However, the case of the HT volcanic eruption is different because the injection altitude was exceptionally high.

Role of H_2O vapor and temperature

Most of the evidence for the occurrence of heterogeneous chemistry in the midlatitude and tropical stratosphere was provided for the tropopause region, where low temperatures are encountered. Modeling studies have indicated the possibility of heterogeneous chemistry occurring on cirrus cloud particles near the midlatitude tropopause (*35*, *36*) or heterogeneous chlorine reactions on liquid sulfate aerosols near tropical monsoon regions (*37*).

Modeling studies have also indicated that enhanced H_2O in the stratosphere could lead to chemical O_3 depletion through heterogeneous chlorine activation and subsequent O_3 destruction (*38*, *39*). Low temperatures (<203 K) and elevated H_2O mixing ratios (>20 ppmv) must be maintained for heterogeneous chlorine activation on sulfate aerosols to occur (*39*).

The largest O_3 loss observed above Réunion Island on 22 January 2022 coincides with H_2O mixing ratios exceeding 100 ppmv at ~25 and 27 km (Fig. 3). Above 25 km, temperature values were 2 to 4 K below the climatological mean temperature profile for January computed using 1998–2021 SHADOZ data for Réunion Island (see the materials and methods). Radiosoundings in the tropics have indicated an average temperature decrease of 2 K caused by the large increase of H_2O vapor after the HT eruption (*14*). Figure 3 shows that O_3 decreases also coincide with the presence of aerosols, as indicated by peaks in the COBALD backscatter measurements. Measurements from an optical particle counter instrument flown that night provide additional information on the aerosol size and concentration, from which aerosol surface area density can be estimated (see the materials and methods). In Fig. 3, the aerosol measurements indicate a peak ambient surface area density of 286.9 $\mu m^2\ cm^{-3}$ at 26.4 km. This is 4 to 6 times higher than what was reported 1 month after the Mt. Pinatubo eruption (*40*) and ~600 times higher than the

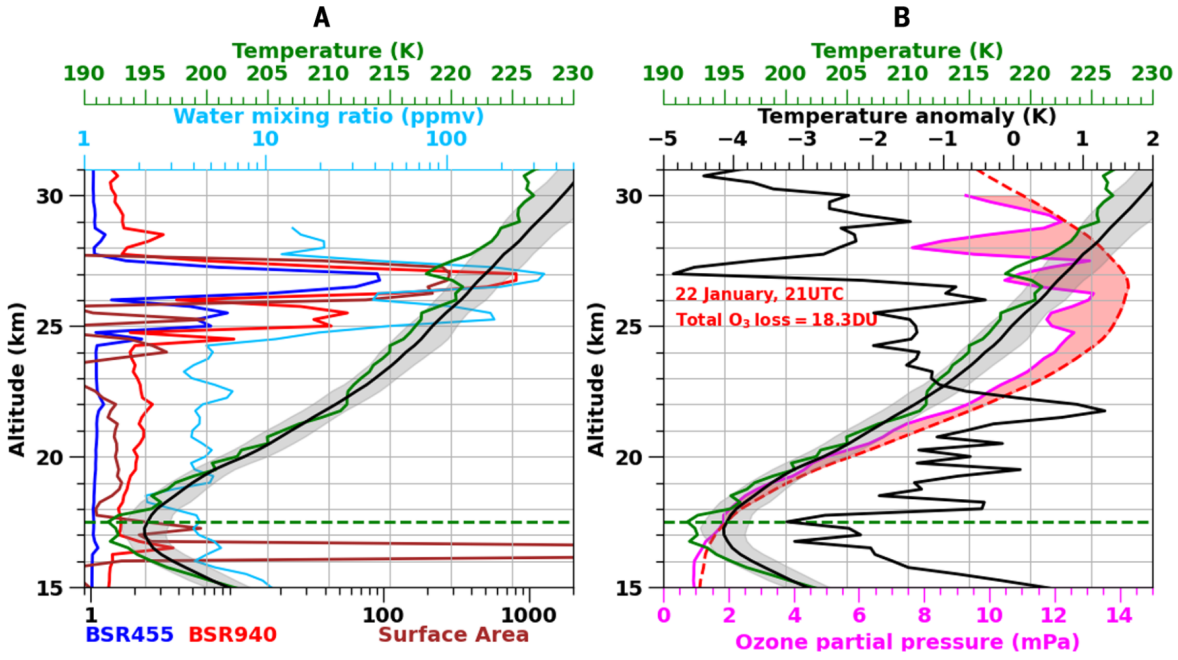

Fig. 3. Soundings at MO on 22 January 2022. (**A** and **B**) Profiles of H_2O vapor mixing ratio (blue), aerosol backscatter ratios at 940 nm (red) and 455 nm (blue), aerosol ambient surface area density (brown, in $\mu m^2\ cm^{-3}$) (A), and O_3 partial pressure (magenta) and temperature (green) (B) measured at MO on 22 January 2022. The horizontal green dashed line shows the location of the tropopause, and the red dashed line shows the O_3 climatology for Réunion Island. The red shaded area illustrates the inferred O_3 loss estimated for that night. The climatological temperature profile for January 1998 to 2021 for Réunion Island is shown in black in (A) and (B); the temperature anomaly from the climatology is shown in (B). The gray shaded area illustrates ±1 SD of the temperature climatology. The average temperature anomaly was −2.2 K between 25 and 30 km.

background stratospheric value of 0.5 μm^2 cm^{-3}. The large humidification of the stratosphere by the HT eruption resulted in rapid aerosol formation in the volcanic plume and in the corresponding large aerosol surface area (*16*).

MLS measurements at 27 km inside the volcanic plume indicate that O_3 decreases (average O_3 anomaly of −0.4 ppmv with decreases as large as −1.5 ppmv) correlated with higher H_2O vapor mixing ratios (mean H_2O of 102 ppmv) and temperatures on average ~2 K below the climatological average (see the materials and methods and fig. S1). Figure 2 shows that a decrease in HCl of 0.4 per million by volume (ppbv) at 28 km corresponds to an increase in ClO of 0.4 ppbv. Low HCl and high ClO reflect the conversion of the halogen reservoir compounds, such as HCl and $ClONO_2$, to the reactive form of chlorine, ClO. Above 25 km, where most of the O_3 loss is observed, it is usually far too warm (>220 K) for heterogeneous chlorine activation to occur (see the materials and methods). However, the large stratospheric humidification, subsequent radiative cooling, and the added surface area after the HT eruption likely accelerated heterogeneous chlorine activation on sulfate aerosols and led to O_3 decreases. To illustrate the impacts of H_2O vapor increase and subsequent radiative cooling on chlorine heterogeneous chemistry, we considered the heterogeneous reactions of $ClONO_2$ + H_2O, $ClONO_2$ + HCl, and HOCl + HCl on sulfate aerosols. The rates of heterogeneous reactions on sulfate aerosols are highly influenced by temperature and H_2O vapor partial pressure, because these factors determine the composition of the sulfate aerosols and the solubility of HCl, $ClONO_2$, and HOCl (*41*).

When H_2O vapor mixing ratios exceed 100 ppmv, the probabilities of the heterogeneous reactions $ClONO_2$ + HCl and HOCl + HCl increase by four orders of magnitude under warm conditions (see the materials and methods and fig. S2). The radiative cooling induced by the large amount of H_2O vapor (−4 K; Fig. 3) can further increase these probabilities by another factor of 10 (see the materials and methods and fig. S2). An increase in H_2O vapor and a corresponding decrease in temperature results in more dilute sulfate aerosols and higher HCl solubility; therefore, the reaction probability for the conversion of HCl to active ClOx (Cl, ClO) increases markedly, and catalytic O_3 loss becomes possible under relatively warm conditions.

Evidence of chlorine activation on hydrated volcanic aerosols

Although the HCl injection into the stratosphere by the HT eruption was comparable to that from previous moderate eruptions observed during the MLS record (*11*), it reached an altitude near 24 km (31.6 hPa) on 16 to 17 January 2022, which is well above levels previously observed by MLS (*11*). In Fig. 2, two main negative HCl anomalies are seen at 24 and 29 km for measurements with large H_2O vapor mixing ratios (>100 ppmv) inside the volcanic plume. The first HCl anomaly value of −0.25 ppbv at 24 km may have been due to scavenging by ice or ash particles (*29*), which were injected up to ~23 km but rapidly washed out within the first day after the eruption (*42*). The second, larger HCl anomaly of −0.4 ppbv at 29 km may indicate HCl heterogeneous activation on sulfate aerosols. Indeed, this negative HCl anomaly coincides with a positive peak of 0.41 ppbv in ClO radicals that is much more pronounced for daytime measurements (Fig. 2). This is consistent with photolysis of Cl_2 and the subsequent reaction of Cl with O_3 to form ClO.

After the HT eruption, elevated H_2O vapor levels reaching at least 70 times the background levels were observed. These increased H_2O concentrations can play a crucial role in enhancing gas-phase chemistry involving HOx radicals, particularly OH and HO_2. The higher H_2O concentrations may boost the HOx cycle, specifically affecting reactions such as OH + O_3 and HO_2 + O_3, which in turn can lead to O_3 depletion. Additionally, the rise in H_2O concentrations strengthens the interaction between the HOx and ClOx cycles (through HO_2 + ClO → HOCl + O_2), with potential implications for O_3 depletion processes (*39*).

A decrease in the observed NO_2 radical abundance indicates slowing of the NO_x cycle, presumably due to N_2O_5 hydrolysis (see the materials and methods and fig. S3). At sunset, the NO_2 concentration is higher than in the morning and better approximates baseline conditions, suggesting that NO_x may at least partially be sustained in the daytime plume. This reduction in NOx can reinforce the ClOx and HOx cycles, contributing to O_3 depletion.

BrO and OClO have been detected in volcanic plumes in the upper troposphere to lower stratosphere region (*43*, *44*), indicating the activation of bromine and chlorine species (because the ClO + BrO reaction is the primary known source of OClO). Li *et al.* (*45*) reported SO_2 and BrO vertical column densities from satellite measurements in the HT volcanic plume for the period 15 to 19 January 2022. Most of the injected BrO spread southeast of the volcano on 16 January 2022, whereas a smaller portion continued to propagate eastward in the subsequent days. Ground-based differential optical absorption spectroscopy (DOAS) observations cannot confirm the presence of elevated BrO in the volcanic plume beyond 19 January 2022 (see the materials and methods), when it was last reported near 130°E in northeastern Australia (*45*). The potential presence of BrO, along with the MLS detection of ClO in the volcanic plume, suggests the possibility of O_3 depletion in the volcanic cloud through the ClO–BrO catalytic cycle (*46*) (see the materials and methods).

Insights from modeling

A recent study by Zhu *et al.* (*47*) used the Whole Atmosphere Community Climate Model (WACCM) to investigate the role of chemistry and transport in O_3 depletion after the HT eruption. The authors simulated the conditions observed by MLS after the eruption by injecting H_2O, ClO (or HCl), and SO_2 into the model. One of their simulations focused on the impact of injecting low O_3, which explained the initial low values observed. However, it was found that these low O_3 levels did not persist over time, suggesting that the injection of tropospheric air poor in O_3 was not a substantial contributing factor. It was also noted that inside the volcanic plume, the concentrations of OH and HO_2 increased by a factor of 10 compared with background levels, with a corresponding enhancement in reaction rates by a factor of 10, specifically for the O_3 loss reactions HO_2 + O_3 and OH + O_3 (see the materials and methods).

Zhu *et al.* also confirmed a large enhancement, by several orders of magnitude, of the heterogeneous reaction rates for $ClONO_2$ + HCl, $ClONO_2$ + H_2O, and HOCl + HCl (see the materials and methods) (*47*). They found that HOCl + HCl was a major cause of chlorine activation. Additionally, they calculated a 20-fold increase in the reaction rate of ClO + HO_2 → HOCl + O_2 (see the materials and methods). The authors also concluded that the massive H_2O injection during the HT eruption led to significant changes in ClOx–HOx interactions and heterogeneous reaction rates, resulting in diverse chemical pathways for chlorine activation and O_3 depletion. HOCl played a crucial role in both in-plume chlorine balance and heterogeneous processes. Both gas-phase chemistry and heterogeneous chemistry are deemed significant factors contributing to O_3 depletion (*47*).

These strengthened ClOx and ClO/HO_2 cycles led to an increase in the O_3 loss reaction Cl + O_3 by a factor of 2, which is sufficient to account for the O_3 loss observed by MLS, even if the contribution from the bromine catalytic cycle is not considered.

Potential mechanisms and impacts on O_3 depletion

The large amount of seawater vaporized during the HT eruption contained sea salt that may have been transported to the stratosphere, providing a source of reactive chlorine, bromine, and iodine species for O_3 destruction. However, it is unclear whether all components of sea salt aerosols would survive wet scavenging in the volcanic plume and be efficiently transported to the stratosphere. Inorganic chlorine (HCl, Cl^-) and bromine (HBr, Br^-) are easily removed by

wet scavenging, whereas inorganic iodine, the dominant form of stratospheric iodine injections, is removed less efficiently (*48*). Even a small injection of iodine into the stratosphere could have accelerated O_3 loss in the volcanic plume because of its much larger O_3-depleting efficiency (*48*–*50*).

Anderson *et al.* (*38*) hypothesized that the excess midlatitude stratospheric H_2O associated with convection changes caused by global warming could destroy lower stratospheric O_3. This HT event appears to be an extreme example of that mechanism. The quantity of H_2O from HT is significantly larger than would be expected from overshooting monsoon convection but provides observational evidence that this process could occur (see the materials and methods). The rapid chemical O_3 loss inside the HT volcanic plume was primarily triggered by the synergistic effects of large humidification, radiative cooling, and added aerosol surface area. All of these effects acted in concert to accelerate HCl heterogeneous activation on sulfate aerosols at warmer temperatures than have been recorded previously. The fact that stratospheric O_3 loss was so rapid after the HT eruption calls for additional experimental studies of heterogeneous chemistry on hydrated aerosols (especially halogen chemistry) to better assess the kinetics of these reactions. It also identifies the need to develop atmospheric modeling tools at finer scales to better understand stratospheric O_3 chemistry in the tropics after extreme events. The increased stratospheric H_2O may linger for 4 to 5 years, potentially altering O_3 chemistry. As noted in Solomon *et al.* (*51*) in regard to the Australian New Year bush fires in 2019–2020, which injected 0.9 Tg of smoke into the stratosphere, there were chemical shifts associated with heterogeneous reactions that altered nitrogen, chlorine and reactive hydrogen species with the potential to cause midlatitude O_3 loss. For the next few years, continued monitoring of O_3, H_2O vapor, aerosols, and halogens is needed to assess the extended impacts of this unprecedented HT eruption.

Methods summary

In situ balloon-borne measurements

Balloon-borne measurements at the MO in Réunion Island in January 2022 included instruments such as the Cryogenic Frost-Point Hygrometer (CFH), the Compact Optical Backscatter and Aerosol Detector (COBALD), the Electrochemical Concentration Cell (ECC) Ozonesonde, SO_2 sonde, and the Portable Optical Particle Counter (POPS). The CFH instrument measures water vapor with an uncertainty of 5 to 10% or less in the stratosphere. COBALD characterizes aerosol particles and clouds based on the backscatter ratio at two wavelengths. ECC Ozonesonde provides O_3 profile data with an uncertainty of 10%. The SO_2 sonde provides SO_2 profile data with an uncertainty of 20%. The Intermet iMet-4-RSB Meteorological Radiosonde supports data telemetering to the ground. POPS measures aerosol size distribution with an uncertainty of 5%. These measurements have a high vertical resolution of 5 m, and all variables were binned in altitude intervals of 100 m to reduce measurement noise.

MLS observations and comparison to high-resolution ozonesonde measurements

The Aura MLS satellite instrument observes thermal emissions from the atmosphere over a wide latitude range. MLS measurements within the volcanic plume were identified by selecting data points with water vapor mixing ratios >10 ppmv and between 100 and 10 hPa. Quality screening criteria were applied to the MLS data to ensure accuracy. To compare high-resolution balloon-borne ozonesonde measurements with MLS data, the sonde data were smoothed to match MLS resolution, and MLS vertical averaging kernels were applied using a priori climatological profiles. Overall, this approach enables the comparison of high-resolution balloon-borne measurements with MLS satellite data while accounting for resolution differences and other factors.

Ozonesonde and SO_2 interference

The presence of SO_2 in the atmosphere can interfere with ECC ozonesonde measurements. ECC ozonesondes measure an electrical current that is produced when O_3 enters the sensor and reacts with KI to produce I within the sonde. By measuring the electron flow and the rate at which O_3 enters the sensor per unit time, the O_3 concentration can be calculated. However, when SO_2 is present, it can convert I^- back into I, leading to lower measured O_3 levels. During the rapid response experiment at MO, SO_2 instruments were launched alongside ECC ozonesondes on some payloads. The 21 January 2022 flight reported that SO_2 interference accounted for ~3 to 4% of the observed O_3 decrease in the ozonesonde profile between 28 and 30 km in altitude.

Zenith-Sky DOAS measurements of stratospheric NO_2

Measurements of stratospheric NO_2 from the University of Colorado DOAS instrument during the plume period (21 January to 1 February 2022) were compared with the clear-sky interannual NO_2 variability for 3 years (January 2020 to January 2022) above MO to assess whether the NOx cycle of stratospheric O_3 destruction was significantly affected by dinitrogen pentoxide (N_2O_5) hydrolysis in the humidified plume. The instrument presents qualitative evidence for a reduction in stratospheric NO_2 during sunrise and sunset, consistent with N_2O_5 hydrolysis, in both geometries overlapping with the plume. However, no evidence for enhanced BrO due to volcanic plume injection was detectable in the DOAS data.

REFERENCES AND NOTES

1. J. H. Seinfeld, S. N. Pandis, *Atmospheric Chemistry and Physics: From Air Pollution to Climate Change* (Wiley, ed. 2, 2006).
2. D. J. Hofmann, S. Solomon, Ozone destruction through heterogeneous chemistry following the eruption of El Chichón. *J. Geophys. Res.* **94**, 5029–5041 (1989). doi: 10.1029/JD094iD04p05029
3. A. Adriani, G. Fiocco, G. P. Gobbi, F. Congeduti, Correlated behavior of the aerosol and ozone contents of the stratosphere after the El Chichon eruption. *J. Geophys. Res.* **92**, 8365–8372 (1987). doi: 10.1029/JD092iD07p08365
4. G. Brasseur, C. Granier, Mount pinatubo aerosols, chlorofluorocarbons, and ozone depletion. *Science* **257**, 1239–1242 (1992). doi: 10.1126/science.257.5074.1239; pmid: 17742756
5. W. J. Randel, F. Wu, J. M. RussellIII, J. W. Waters, L. Froidevaux, Ozone and temperature changes in the stratosphere following the eruption of Mount Pinatubo. *J. Geophys. Res.* **100**, 16753–16764 (1995). doi: 10.1029/95JD01001
6. J. K. Angell, Estimated impact of Agung, El Chichon and Pinatubo volcanic eruptions on global and regional total ozone after adjustment for the QBO. *Geophys. Res. Lett.* **24**, 647–650 (1997). doi: 10.1029/97GL00544
7. M. R. Schoeberl, P. K. Bhartia, E. Hilsenrath, O. Torres, Tropical ozone loss following the eruption of Mt. Pinatubo. *Geophys. Res. Lett.* **20**, 29–32 (1993). doi: 10.1029/92GL02637
8. W. B. Grant *et al.*, Observations of reduced ozone concentrations in the tropical stratosphere after the eruption of Mt. Pinatubo. *Geophys. Res. Lett.* **19**, 1109–1112 (1992). doi: 10.1029/92GL01153
9. J.-P. Vernier *et al.*, VolKilau: Volcano Rapid Response Balloon Campaign during the 2018 Kilauea Eruption. *Bull. Am. Meteorol. Soc.* **101**, E1602–E1618 (2020). doi: 10.1175/BAMS-D-19-0011.1
10. S. A. Carn, N. A. Krotkov, B. L. Fisher, C. Li, Out of the blue: Volcanic SO2 emissions during the 2021–2022 eruptions of Hunga Tonga—Hunga Ha'apai (Tonga). *Front. Earth Sci. (Lausanne)* **10**, 976962 (2022). doi: 10.3389/feart.2022.976962
11. L. Millán *et al.*, The Hunga Tonga-Hunga Ha'apai Hydration of the Stratosphere. *Geophys. Res. Lett.* **49**, GL099381 (2022). doi: 10.1029/2022GL099381; pmid: 35865735
12. G. J. S. Bluth, S. D. Doiron, C. C. Schnetzler, A. J. Krueger, L. S. Walter, Global tracking of the SO_2 clouds from the June, 1991 Mount Pinatubo eruptions. *Geophys. Res. Lett.* **19**, 151–154 (1992). doi: 10.1029/91GL02792
13. W. G. Read, L. Froidevaux, J. W. Waters, Microwave limb sounder measurement of stratospheric SO_2 from the Mt. Pinatubo Volcano. *Geophys. Res. Lett.* **20**, 1299–1302 (1993). doi: 10.1029/93GL00831
14. H. Vömel, S. Evan, M. Tully, Water vapor injection into the stratosphere by Hunga Tonga-Hunga Ha'apai. *Science* **377**, 1444–1447 (2022). doi: 10.1126/science.abq2299; pmid: 36137033
15. J.-L. Baray *et al.*, Maïdo Observatory: A new high-altitude station facility at Reunion Island (21° S, 55° E) for long-term atmospheric remote sensing and in situ measurements. *Atmos. Meas. Tech.* **6**, 2865–2877 (2013). doi: 10.5194/amt-6-2865-2013
16. Y. Zhu *et al.*, Perturbations in stratospheric aerosol evolution due to the water-rich plume of the 2022 Hunga-Tonga eruption. *Commun. Earth Environ.* **3**, 248 (2022). doi: 10.1038/s43247-022-00580-w
17. J. G. Anderson, D. M. Wilmouth, J. B. Smith, D. S. Sayres, UV dosage levels in summer: Increased risk of ozone loss from convectively injected water vapor. *Science* **337**, 835–839 (2012). doi: 10.1126/science.1222978; pmid: 22837384
18. S. Yoon *et al.*, Development and testing of a novel sulfur dioxide sonde. *Atmos. Meas. Tech.* **15**, 4373–4384 (2022). doi: 10.5194/amt-15-4373-2022
19. J. W. Waters *et al.*, The Earth Observing System Microwave Limb Sounder (EOS MLS) on the Aura satellite. *IEEE Trans. Geosci. Remote Sens.* **44**, 1075–1092 (2006). doi: 10.1109/TGRS.2006.873771
20. N. J. Livesey *et al*, "EOS MLS version 4.2x level 2 data quality and description document (revision E)" (Technical Report, Jet Propulsion Laboratory, NASA, 2020); https://mls.jpl.nasa.gov/data/v4-2_data_quality_document.pdf

21. P. Sellitto *et al*., The unexpected radiative impact of the Hunga Tonga eruption of 15th January 2022. *Commun. Earth Environ.* **3**, 288 (2022). doi: 10.1038/s43247-022-00618-z
22. S. Solomon, Stratospheric ozone depletion: A review of concepts and history. *Rev. Geophys.* **37**, 275–316 (1999). doi: 10.1029/1999RG900008
23. N. J. Livesey, M. L. Santee, G. L. Manney, A Match-based approach to the estimation of polar stratospheric ozone loss using Aura Microwave Limb Sounder observations. *Atmos. Chem. Phys.* **15**, 9945–9963 (2015). doi: 10.5194/acp-15-9945-2015
24. B. J. Johnson *et al*., South Pole Station ozonesondes: Variability and trends in the springtime Antarctic ozone hole 1986–2021. *Atmos. Chem. Phys.* **23**, 3133–3146 (2023). doi: 10.5194/acp-23-3133-2023
25. D. J. Lary, Catalytic destruction of stratospheric ozone. *J. Geophys. Res.* **102**, 21515–21526 (1997). doi: 10.1029/97JD00912
26. R. J. Salawitch, Sensitivity of ozone to bromine in the lower stratosphere. *Geophys. Res. Lett.* **32**, L05811 (2005). doi: 10.1029/2004GL021504
27. M. A. Tolbert, M. J. Rossi, D. M. Golden, Heterogeneous interactions of chlorine nitrate, hydrogen chloride, and nitric acid with sulfuric acid surfaces at stratospheric temperatures. *Geophys. Res. Lett.* **15**, 847–850 (1988). doi: 10.1029/GL015i008p00847
28. C. Textor, Injection of gases into the stratosphere by explosive volcanic eruptions. *J. Geophys. Res.* **108**, 4606 (2003). doi: 10.1029/2002JD002987
29. A. Tabazadeh, R. P. Turco, Stratospheric chlorine injection by volcanic eruptions: HCl scavenging and implications for ozone. *Science* **260**, 1082–1086 (1993). doi: 10.1126/science.260.5111.1082; pmid: 17806335
30. J. Staunton-Sykes *et al*., Co-emission of volcanic sulfur and halogens amplifies volcanic effective radiative forcing. *Atmos. Chem. Phys.* **21**, 9009–9029 (2021). doi: 10.5194/acp-21-9009-2021
31. C. Granier, G. Brasseur, Impact of heterogeneous chemistry on model predictions of ozone changes. *J. Geophys. Res.* **97**, 18015–18033 (1992). doi: 10.1029/92JD02021
32. M. Prather, Catastrophic loss of stratospheric ozone in dense volcanic clouds. *J. Geophys. Res.* **97**, 10187–10191 (1992). doi: 10.1029/92JD00845
33. M. Kilian, S. Brinkop, P. Jöckel, Impact of the eruption of Mt Pinatubo on the chemical composition of the stratosphere. *Atmos. Chem. Phys.* **20**, 11697–11715 (2020). doi: 10.5194/acp-20-11697-2020
34. V. Aquila, L. D. Oman, R. S. Stolarski, P. R. Colarco, P. A. Newman, Dispersion of the volcanic sulfate cloud from a Mount Pinatubo–like eruption. *J. Geophys. Res.* **117**, D06216 (2012). doi: 10.1029/2011JD016968
35. S. Borrmann, S. Solomon, L. Avallone, D. Toohey, D. Baumgardner, On the occurrence of ClO in cirrus clouds and volcanic aerosol in the tropopause region. *Geophys. Res. Lett.* **24**, 2011–2014 (1997). doi: 10.1029/97GL02053
36. S. Solomon *et al*., Heterogeneous chlorine chemistry in the tropopause region. *J. Geophys. Res.* **102**, 21411–21429 (1997). doi: 10.1029/97JD01525
37. S. Solomon *et al*., Monsoon circulations and tropical heterogeneous chlorine chemistry in the stratosphere. *Geophys. Res. Lett.* **43**, (2016). doi: 10.1002/2016GL071778
38. J. G. Anderson *et al*., Stratospheric ozone over the United States in summer linked to observations of convection and temperature via chlorine and bromine catalysis. *Proc. Natl. Acad. Sci. U.S.A.* **114**, E4905–E4913 (2017). doi: 10.1073/pnas.1619318114; pmid: 28584119
39. S. Robrecht *et al*., Mechanism of ozone loss under enhanced water vapour conditions in the mid-latitude lower stratosphere in summer. *Atmos. Chem. Phys.* **19**, 5805–5833 (2019). doi: 10.5194/acp-19-5805-2019
40. T. Deshler, D. J. Hofmann, B. J. Johnson, W. R. Rozier, Balloonborne measurements of the Pinatubo aerosol size distribution and volatility at Laramie, Wyoming during the summer of 1991. *Geophys. Res. Lett.* **19**, 199–202 (1992). doi: 10.1029/91GL02787
41. D. R. Hanson, A. R. Ravishankara, S. Solomon, Heterogeneous reactions in sulfuric acid aerosols: A framework for model calculations. *J. Geophys. Res.* **99**, 3615–3629 (1994). doi: 10.1029/93JD02932
42. B. Legras *et al*., The evolution and dynamics of the Hunga Tonga–Hunga Ha'apai sulfate aerosol plume in the stratosphere. *Atmos. Chem. Phys.* **22**, 14957–14970 (2022). doi: 10.5194/acp-22-14957-2022
43. N. Theys *et al*., Global observations of tropospheric BrO columns using GOME-2 satellite data. *Atmos. Chem. Phys.* **11**, 1791–1811 (2011). doi: 10.5194/acp-11-1791-2011
44. C. Hörmann *et al*., Systematic investigation of bromine monoxide in volcanic plumes from space by using the GOME-2 instrument. *Atmos. Chem. Phys.* **13**, 4749–4781 (2013). doi: 10.5194/acp-13-4749-2013
45. Q. Li *et al*., Diffusion height and order of sulfur dioxide and bromine monoxide plumes from the Hunga Tonga–Hunga Ha'apai volcanic eruption. *Remote Sens. (Basel)* **15**, 1534 (2023). doi: 10.3390/rs15061534
46. M. B. McElroy, R. J. Salawitch, S. C. Wofsy, J. A. Logan, Reductions of Antarctic ozone due to synergistic interactions of chlorine and bromine. *Nature* **321**, 759–762 (1986). doi: 10.1038/321759a0
47. Y. Zhu *et al*., "Stratospheric ozone depletion inside the volcanic plume shortly after the 2022 Hunga Tonga eruption" (EGUsphere, 2023); https://doi.org/10.5194/egusphere-2023-1334.
48. T. K. Koenig *et al*., Quantitative detection of iodine in the stratosphere. *Proc. Natl. Acad. Sci. U.S.A.* **117**, 1860–1866 (2020). doi: 10.1073/pnas.1916828117; pmid: 31932452
49. World Meteorological Organization, "Scientific assessment of ozone depletion: 2018" (WMO, 2018), Global Ozone Research and Monitoring Project, Report No. 58; https://csl.noaa.gov/assessments/ozone/2018/.
50. L. J. Carpenter *et al*., "Update on ozone-depleting substances (ODSs) and other gases of interest to the Montreal Protocol," in *Scientific Assessment of Ozone Depletion: 2014* (World Meteorological Organization, 2014), Global Ozone Research and Monitoring Project Report No. 55; https://www.nist.gov/publications/update-ozone-depleting-substances-odss-and-other-gases-interest-montreal-protocol.
51. S. Solomon *et al*., On the stratospheric chemistry of midlatitude wildfire smoke. *Proc. Natl. Acad. Sci. U.S.A.* **119**, e2117325119 (2022). doi: 10.1073/pnas.2117325119; pmid: 35238658
52. CFH ozonesonde data for: S. Evan *et al*., Rapid ozone depletion after humidification of the stratosphere by the Hunga Tonga Eruption, GeoNetwork (2023); https://doi.org/10.26171/p4zy-fy98.
53. ECC ozonesonde data for: S. Evan *et al*., Rapid ozone depletion after humidification of the stratosphere by the Hunga Tonga Eruption, GeoNetwork (2023); https://doi.org/10.26171/mvee-5v84.
54. Raw MLS H_2O data for: S. Evan *et al*., Rapid ozone depletion after humidification of the stratosphere by the Hunga Tonga Eruption, GES DISC (2023); https://disc.gsfc.nasa.gov/datasets/ML2H2O_004/summary?keywords=aura.
55. Raw MLS O_3 data for: S. Evan *et al*., Rapid ozone depletion after humidification of the stratosphere by the Hunga Tonga Eruption, GES DISC (2023); https://disc.gsfc.nasa.gov/datasets/ML2O3_004/summary?keywords=aura.
56. Raw MLS HCl data for: S. Evan *et al*., Rapid ozone depletion after humidification of the stratosphere by the Hunga Tonga Eruption, GES DISC (2023); https://disc.gsfc.nasa.gov/datasets/ML2HCL_004/summary?keywords=aura.
57. Raw MLS ClO data for: S. Evan *et al*., Rapid ozone depletion after humidification of the stratosphere by the Hunga Tonga Eruption, GES DISC (2023); https://disc.gsfc.nasa.gov/datasets/ML2CLO_004/summary?keywords=aura.

ACKNOWLEDGMENTS

We thank G. Morris, D. Murphy, M. Abou-Ghane, and J. Burkholder for discussions; A. Wong, T. Koenig, C. Thompson, and SilverLining for support; and the European Communities, the Région Réunion, CNRS, and Université de la Réunion for support and contributions in the construction phase of the research infrastructure Observatoire de Physique de l'Atmosphère de La Réunion, including Maïdo Observatory (OPAR). OPAR is presently funded by CNRS (INSU), Météo France, and Université de La Réunion and managed by OSU-R (Observatoire des Sciences de l'Univers de La Réunion, UAR 3365). **Funding:** This work was supported by the Agence Nationale de la Recherche (ANR CONCIRTO award ANR-17-CE01-0005-01), the National Science Foundation (NSF awards AGS-1620530 and AGS-2027252), and the National Aeronautics and Space Administration (NASA contract 80NM0018D0004). **Author contributions:** Conceptualization: S.E.; Data curation: S.E., J.B., R.V., C.F.L., J.M.M., K.L., P.W., S.L.A., J.H.F., E.A., L.A., M.T., H.V., F.G.W., L.M., M.L.S., L.F., W.G.R.; Methodology: S.E., J.B.; Writing – original draft: all authors. Writing – review & editing: all authors. **Competing interests:** The authors declare no competing interests. **Data and materials availability:** The processed CFH (*52*) and ECC (*53*) ozonesonde data used in this study are available at GeoNetwork. Raw MLS H_2O (*54*), O_3 (*55*), HCl (*56*), and ClO (*57*) data may be found at the NASA Goddard Earth Sciences Data and Information Services Center (GES DISC) repository.

SUPPLEMENTARY MATERIALS

science.org/doi/10.1126/science.adg2551
Materials and Methods
Figs. S1 to S3
Table S1
References (*58*–*86*)

Submitted 12 December 2022; accepted 5 September 2023
10.1126/science.adg2551